# Infrared Optical Constants of Coal Slags: Dependence on Chemical Composition

D. G. Goodwin* and M. Mitchner†
*Stanford University, Stanford, California*

**The results of an experimental study of the infrared optical constants of coal slags are presented. The real and imaginary parts of the refractive index were determined from transmittance and reflectance measurements carried out on thin polished glassy slag wafers at room temperature from visible wavelengths to 13 μm. The dependence of the optical constants on slag chemical composition was investigated, and correlations were developed based on the measured data to allow estimation of the optical constants as a function of wavelength and composition.**

## Introduction

THE presence of mineral matter in coal has several consequences for radiative heat transfer in coal combustion systems. The fly-ash particles dispersed in the combustion gases may absorb, emit, and scatter radiation, with possibly significant effects on heat transfer.[1,2] Also, the slag layers formed on the walls alter the wall radiative properties.

To estimate the effects of either fly ash or slag layers (which may be semitransparent[3]) on radiative heat transfer, one needs data on the complex refractive index $m = n - ik$ of the ash/slag at infrared wavelengths. For calculations of radiant emission by the fly ash, the imaginary part $k$ of the refractive index is of particular importance. At present, the available data on the optical constants (i.e., $n$ and $k$) are fairly sparse and uncertain, particularly on $k$. Although there have been several reported measurements of $n$ and $k$ for fly ash,[4-9] in each case, experimental problems were encountered that appear to have significantly affected the measured values.

The earliest reported optical constants for fly ash by Willis[4] were later shown by Gupta and Wall[10] to be in error from the use of incorrect data-reduction procedures. Similarly, the experimental technique used by Volz[5] to measure $k$ for fly ash was later shown by Toon et al.[11] to be inapplicable for particles in the size range of fly-ash particles as a result of neglect of scattering.

Lowe et al.[6] and Gupta and Wall[8] measured $k$ for fly ash in situ in an operating pulverized coal utility boiler. In both studies, however, the measured values were biased by the presence of up to 10% residual carbon in the ash at the measurement location.[8] Cowen et al.[7] found similar effects of residual carbon in their measurements of $k$ on sampled submicron ash. Finally, Wyatt[9] has reported optical constants for fly-ash particles at a wavelength of 0.6328 μm, measured using a single-particle light-scattering technique. A later sensitivity analysis of the technique by Marx,[12] however, concluded that the method cannot be used reliably to measure $k$ for values below 0.01 (which is greater than the values reported by Wyatt) although it can be used to measure $n$ accurately.

In light of the problems encountered in the studies to date, it is clear that there is a need for improved data on the optical constants of fly ash in the infrared. Unfortunately, considerations of the experimental problems involved[13] and the experience of others[14,15] who have attempted measurements on similar types of particles (e.g., atmospheric or interstellar dust) suggest that it ill be very difficult, if at all possible, to measure directly accurate infrared $k$ values for fly ash with currently used experimental techniques. Although there are many problems encountered in such measurements (e.g., particle agglomeration and carbon contamination), the primary difficulty is scattering: At visible or near-infrared wavelengths, fly-ash particles are nearly transparent and thus scatter much more strongly than they absorb. In practice, accounting quantitatively for the effects of scattering in a measurement of $k$ is extremely difficult. A comparative study by Gerber and Hindman[14] of techniques for measuring the optical constants of particulates showed that all approaches strongly overestimate $k$ for weakly absorbing, strongly scattering particles.

Furthermore, since fly ash consists of a mixture of particles with different compositions, all measurement techniques other than the single particle techniques result in "average" optical constants. As first pointed out by Bergstrom,[16] the use of average optical constants may lead to significant errors in radiative transfer calculations. A preferable approach is to account explicitly for the mixture of particle types, averaging the computed cross sections (rather than the optical constants) over composition.[13] Thus, the utility of optical constants measured directly on a large sample of fly-ash particles may be questioned, even apart from the above-mentioned experimental difficulties.

Considering the significant problems associated with making accurate optical measurements on fly-ash particles, it is worth considering alternatives. Fortunately, it appears that good estimates of the absorption and scattering properties of fly-ash dispersions can be made without requiring that the optical constants be determined by direct measurements on fly ash. The ability to follow this approach rests on the fact that fly-ash particles are primarily glass-like spheres and, thus, their absorption and scattering efficiencies may be calculated from Lorenz-Mie theory using optical constants for the bulk glass, provided these are known for the relevant composition. The contribution to the absorption and scattering coefficients of the dispersion due to the small quantities of other types of particles present in ash (e.g., iron oxides, silica, and carbonaceous particles) may be accounted for separately, since the optical constants of these components are known or may be reasonably estimated.

This approach requires information on the distribution of chemical compositions within the ash, which may be obtained with electron microprobe techniques.[17,18] It also requires knowing the optical constants of glasses similar in composition to fly-ash particles, for the wavelength range of interest for radiative heat-transfer calculations (≈ 1-12 μm), including data on the variation with chemical composition and temperature.

Received Nov. 30, 1987; revision received March 14, 1988. 

*Research Assistant, High Temperature Gasdynamics Laboratory, Department of Mechanical Engineering; currently at Department of Mechanical Engineering, California Institute of Technology, Pasadena, CA.

†Professor (Emeritus), High Temperature Gasdynamics Laboratory, Department of Mechanical Engineering. Member AIAA.

The qualitative features of infrared absorption in glasses are well known.[19] At relatively short wavelengths (less than about 4 $\mu$m), absorption is due largely to the presence of transition metal impurities in the glass (e.g., iron and titanium in the case of fly ash) and is sensitive to the oxidation state in which the transition metal ion occurs. For example, the $Fe^{2+}$ ion absorbs in the infrared, but the $Fe^{3+}$ ion does not.[20] At longer wavelengths, a series of strong vibrational absorption peaks are seen that dominate the optical properties in this spectral region. Of particular note is the strong Si-O vibrational peak, which is found near 9 $\mu$m in a wide range of Si-bearing crystals and glasses.[19]

Although the absorption mechanisms are qualitatively understood, quantitative data on the infrared optical constants of relevant glasses are severely lacking. With one exception,[21] there have been no studies to date on glasses with compositions reasonably similar to those of fly ash. In particular, all studies of absorption by transition metals in glasses have been limited to glasses with Fe concentrations much lower than those that are of interest for fly-ash/slag studies.

In the present paper, we present the results of an experimental study of the optical constants of bulk glassy materials with compositions similar to fly ash. (We will use the term "slag" to denote all such materials.) The dependence of the optical constants on chemical composition was investigated, and correlations were developed to predict $n$ and $k$ as a function of composition and wavelength, over the wavelength range of $\approx 0.7$–$13$ $\mu$m.

The results given here are limited to measurements made at room temperature. Measurements were also made of the temperature dependence of $k$ for temperatures up to 1200 K, but these results will be published separately. (A complete account of this work is available in the thesis by Goodwin.[22])

## Experimental Procedure

A set of glassy synthetic slag samples for the measurements was prepared first by heating mixtures of reagent-grade oxide powders in a laboratory furnace (Deltec model DT31) to form molten slags, which were then cooled to room temperature to yield glassy samples. A "base" composition was chosen as 58% $SiO_2$, 29% $Al_2O_3$, and 13% CaO (by weight), to which various amounts of $Fe_2O_3$ and/or $TiO_2$ were added. This composition was chosen to be representative of ash compositions,[23] while also insuring a composition that could be melted at an attainable furnace temperature ($<1700°C$).

The melts were carried out under controlled atmospheric conditions. An alumina tube running vertically through the furnace and containing the melt crucible was purged either with air or with one of three $CO$:$CO_2$:$N_2$ mixtures, with $CO$:$CO_2$ molar ratios of 0.1, 1.0, and 10.0, respectively. In this manner, slags with a range of oxidation states, from fully reduced to moderately oxidized, were prepared.

Platinum crucibles (10-cc. capacity) were used to contain the melts in oxidizing environments, and alumina crucibles in reducing environments. The melts were held at a temperature of $\approx 1560°C$ for up to 24 h (only 8 h with the alumina crucibles) to attempt to approach $Fe^{2+} - Fe^{3+}$ equilibration. The melts were then cooled to room temperature at a relatively slow rate of 6°C/min, to obtain samples free enough of microcracks to allow them to be sliced into thin wafers.

For the slags prepared in reducing environments, a crystalline portion was often found at the bottom of the crucible. The demarcation between this crystalline region and the glassy region above was always distinct. The glassy and crystalline portions were carefully separated from one another, and only the glassy portion was used for the measurements.

In most cases, two wafers were prepared from each slag sample, with different thicknesses. The thicker wafer was in each case cut to 500 $\mu$m, and the thinner wafer to either 50 or 100 $\mu$m. The wafers were then polished to optical quality (in most cases specified as $\lambda/4$, where $\lambda$ is a visible wavelength). With these two wafers for each slag, it was possible to make transmittance measurements from ultraviolet wavelengths to 8 $\mu$m in the infrared.

In addition to the "synthetic" slags prepared in this manner, three "natural" slags were prepared by remelting collected fly ash or slag. Preliminary results of this work for these three natural slags have been discussed previously.[24]

The elemental compositions of the prepared slags were determined by electron microprobe measurements carried out directly on the wafer surfaces. The $Fe^{2+}/Fe^{3+}$ ratio (i.e., oxidation state) was measured using the Mössbauer spectroscopic technique.[25]

A total of 16 synthetic slags were prepared, with $Fe_2O_3$ contents ranging from 0.0% to 17.86% by weight. Then, $TiO_2$ was added to 4 slags, with a maximum value of 1.27% by weight. The $Fe^{2+}/(Fe^{2+} + Fe^{3+})$ ratios ranged from a low of 0.558 for a sample prepared in air, to 1.0 for 2 samples prepared in reducing environments.

The transmittance and near-normal reflectance spectra of the wafers were measured, from which the optical constants were determined. The infrared room-temperature transmittance and reflectance measurements used the optical system described previously,[24] with minor improvements. Visible and UV transmittance measurements were made using a commercial spectrophotometer (Perkin-Elmer model 330). At room temperature, the transmittance measurements were made from a minimum wavelength of 190 nm (for the Fe-free slag) to a maximum wavelength of 8 $\mu$m. The reflectance measurements were made from 1 to 13 $\mu$m. At wavelengths where both transmittance and reflectance measurements were made, the optical constants were determined directly from the appropriate relations from electromagnetic theory for the transmittance/reflectance of a plane-parallel slab.[13] At wavelengths beyond 8 $\mu$m, the optical constants were determined from a Kramers-Kronig analysis of the measured reflectance spectrum.[22,24] The two techniques agreed well near 8 $\mu$m, where both could be used. For wavelengths below 1 $\mu$m, only $k$ was determined, using the value of $n$ measured at 1 $\mu$m for the (relatively minor) surface-reflection correction.

The relative error in the measured transmittance and reflectance values was estimated to be less than 2% (i.e., $\Delta T/T < 0.02$). The transmittance measurement error usually contributed little to the uncertainty in $k$ because of the logarithmic dependence of $k$ on the measured transmittance. The error in $k$ was generally dominated by the uncertainty in the wafer thickness (2%). The error in $n$ was tested by making measurements for pure samples of fused silica and sapphire in the wavelength range 1–1.5 $\mu$m. For fused silica, the largest relative error in $n$ was 0.33%; for sapphire, the largest error was 0.6% (1.15%), using the literature $n$ values[26] for the extraordinary (ordinary) ray. At wavelengths where $n$ and $k$ were determined using the Kramers-Kronig technique, the error in the computed reflection phase angle yields an uncertainty in both $n$ and $k$ of $\approx \pm 0.1$.

## Results and Discussion

### Overview of Measured Optical Constants

Typical measured optical constants are shown in Fig. 1, which illustrates the major features observed for all of the slag samples. The chemical compositions of these samples are given in Table 1. Considering first the Fe-free sample SA00, it is seen that $k$ exhibits a strong wavelength dependence, varying by more than 5 orders of magnitude over the wavelength range shown. The minimum $k$ value for this sample is less than $10^{-5}$, and the maximum is $\approx 1.0$. As will be discussed later, virtually all of the features in the $k$ spectrum for this sample are attributable to its silica content, including the large peak near 9 $\mu$m, the shoulder region from 5–8 $\mu$m, and the rise in $k$ near 13 $\mu$m. (The UV absorption, however, is caused by trace amounts of Fe.) The other elements present in the sample have only very minor effects on $k$ in this wavelength range.

The Fe-bearing slags show substantially greater $k$ values in the wavelength region $\lambda < 4$ μm, although the values at longer wavelengths are nearly identical to those of the Fe-free sample. The fully reduced slag (SE10) exhibits greater absorption in the 1-4 μm region than does the mixed oxidation state sample (SA10), even though its total $Fe_2O_3$ content is somewhat less. At visible wavelengths, however, sample SA10 shows much greater absorption. These effects may be understood in terms of the absorption mechanisms of iron ions in minerals and glasses,[27] which will be discussed in more detail later.

The $k$ spectrum for the "natural" slag NA01, formed from remelted fly ash, shows two features not seen in the synthetic slag spectra. A small absorption band appears near 2.8 μm, and a larger one near 7 μm. The band at 2.8 μm is often seen in the infrared absorption spectrum of glasses and may be identified as the stretching vibration of OH. The band at 7 μm has apparently not been previously identified in a glass (owing to the general lack of measurements in this spectral region) but may be identified as the bending vibration of OH by comparison to the spectra of OH-bearing organic molecules (e.g., alcohols).[28] The presence of OH bound within the slag is a consequence of the large amount of OH-bearing clay minerals present in coal. Aside from these two bands, the results for this sample are quite similar to those for the synthetic slags.

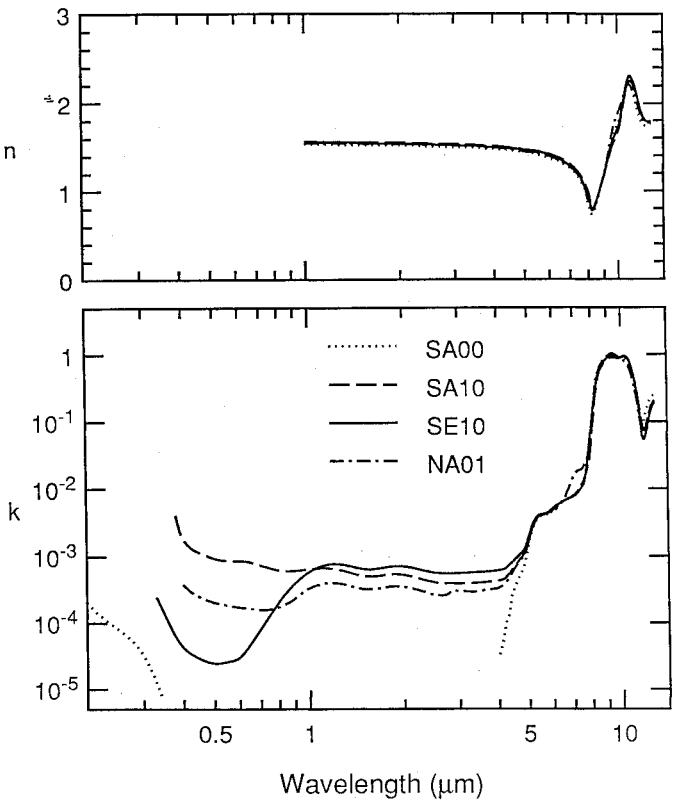


**Fig. 1 Typical measured optical constants. The chemical compositions of these slags are given in Table 1.**

**Table 1 Chemical compositions of the subset of slags discussed in this paper[a]**

| | SA00 | SA10 | SB20 | SE10 | NA01 |
|---|---|---|---|---|---|
| $SiO_2$ | 56.16 | 50.64 | 45.97 | 53.70 | 55.24 |
| $Al_2O_3$ | 27.54 | 25.04 | 22.59 | 23.45 | 22.17 |
| CaO | 16.26 | 14.82 | 13.57 | 14.42 | 10.83 |
| $Fe_2O_3$ | 0.04 | 9.51 | 17.86 | 8.42 | 5.68 |
| $TiO_2$ | 0.00 | 0.00 | 0.00 | 0.00 | 1.01 |
| MgO | 0.00 | 0.00 | 0.00 | 0.00 | 1.96 |
| $K_2O$ | 0.00 | 0.00 | 0.00 | 0.00 | 1.58 |
| $Na_2O$ | 0.00 | 0.00 | 0.00 | 0.00 | 0.30 |
| $P_2O_5$ | 0.00 | 0.00 | 0.00 | 0.00 | 1.22 |
| $[Fe^{2+}]/([Fe^{2+}] + [Fe^{3+}])$ | – | 0.56 | 0.66 | 1.0 | 0.77 |

[a]Oxide values are percent by weight.

The real part of the refractive index shows the general behavior one would expect. The value of $n$ at $\lambda = 1$ μm is near 1.5 and then decreases with increasing wavelength. In the long wavelength region, $n$ exhibits a dispersion profile associated with the peak in $k$ in this wavelength range.

The measured optical constants are in good qualitative agreement with those given by Pollack et al.[21] for two naturally occurring samples (obsidian and basaltic glass) that had compositions similar to the slags investigated here. The structure in the $k$ spectrum in the 5-8 μm range was, however, not resolved in the measurements of Ref. 21 because of the use of an experimental technique for $\lambda > 5$ μm that cannot measure $k$ values below 0.1.

### Composition Dependence of the Optical Constants

A primary goal of this work was to investigate the quantitative dependence of $n$ and $k$ on the chemical composition of the slag. A mixture rule was developed to allow calculation of $n$ as a function of composition in the wavelength range 1-8 μm. Also, a correlation for the dependence of $k$ on Fe content and oxidation state was developed for the wavelength range 0.75-4 μm. Finally, a damped-harmonic-oscillator model is presented for the long-wavelength region 8-13 μm.

The mixture rule for $n$ assumes that the refractivity

$$R = (n^2 - 1)/(n^2 + 2) \tag{1}$$

is a linear function of composition, as is often done.[29] If the composition is expressed on a mass fraction basis, the value of $n$ for the slag may be written as

$$\frac{n^2 - 1}{n^2 + 2} = \rho \sum_i \left(\frac{X_{m,i}}{\rho_i}\right)\left(\frac{n_i^2 - 1}{n_i^2 + 2}\right) \tag{2}$$

where $\rho$ is the sample density, $X_{m,i}$ the mass fraction of component $i$ in the slag, and $\rho_i$ and $n_i$ the density and refractive index, respectively, for component $i$ in a pure "reference" state, for which refractive index data are available. The slag components are taken to be the oxides $SiO_2$, $Al_2O_3$, CaO, $Fe_2O_3$, $TiO_2$, and MgO. The reference states of these oxides are assumed to be fused silica, sapphire, crystalline CaO, hematite, rutile, and crystalline MgO, respectively. The refractive index values for these minerals were taken from the literature[30-34] and were fit to simplified dispersion equations of the form

$$n_i^2 - 1 = C_i + (B_i \lambda^2)/(\lambda^2 - \lambda_{0,i}^2) \tag{3}$$

The values of the three parameters $B_i$, $C_i$, and $\lambda_{0,i}$ in Eq. (3) are given in Table 2 for each oxide component, along with the density in the reference state. It should be noted that owing to insufficient experimental data, the value of $n$ for $Fe_2O_3$ is taken to be independent of wavelength and equal to its value at visible wavelengths.

The sample density also appears in Eq. (2). The density was measured for several of the present slags, and the correlation

$$\rho = 2.54 + 0.00978\ (Fe_2O_3) \quad g/cm^3 \tag{4}$$

**Table 2 Dispersion equation parameters for pure oxides**

| Oxide | Density, g/cm³ | $C_i$ | $B_i$ | $\lambda_{0,i}$, μm |
|---|---|---|---|---|
| $SiO_2$ | 2.20 | 1.104 | 0.8975 | 9.896 |
| $Al_2O_3$ | 3.97 | 2.082 | 5.281 | 17.93 |
| CaO | 3.31 | 2.31 | 11.32 | 33.90 |
| $Fe_2O_3$ | 5.24 | 8.364 | 0.0 | 0.0 |
| $TiO_2$ | 4.86 | 5.031 | 7.764 | 15.60 |
| MgO | 3.58 | 1.962 | 2.470 | 15.56 |

was found to fit the measured values to within 0.5%, where $(Fe_2O_3)$ denotes the weight percent $Fe_2O_3$. This expression was used in all cases for $\rho$ in Eq. (2).

The comparison between the measured values of $n$ and those predicted by Eqs. (2–4) is shown in Fig. 2. The dashed curves show the computed values, and the points the measured values. In general, the agreement is quite good, particularly considering that Eq. (2) is based solely on data for the pure oxides, with no adjusted constants. The relative effect of $Fe_2O_3$ on $n$ is clearly well predicted by the mixture rule throughout this wavelength range, despite its relatively crude treatment (wavelength-independent $n$).

The value of $n$ predicted by Eqs. (2–4) is, however, consistently slightly low. It was found that the mixture rule could be substantially improved by making two empirical adjustments. The right-hand side of Eq. (2) was multiplied by an overall factor of 1.032, and the value of $\lambda_0$ for $SiO_2$ was increased by 0.22 $\mu$m. These values were arrived at by minimizing the least-squares error between the predicted and measured values, summed over all samples. The predictions of the modified mixture rule are shown as the solid lines in Fig. 2.

By substituting from Eq. (3) for $n_i$ in Eq. (2), the final mixture rule for $n$ may be written in the form

$$\frac{n^2-1}{n^2+2} = \rho \sum_i X_{m,i} F_i(\lambda) \tag{5}$$

where

$$F_i(\lambda) = (a_i\lambda^2 - b_i)/(c_i\lambda^2 - d_i) \tag{6}$$

The values of the parameters $a_i$, $b_i$, $c_i$, and $d_i$, including the two empirical corrections, are given in Table 3.

The correlation for the effects of Fe on the imaginary part $k$ of the refractive index was developed by considering the two absorption mechanisms by which Fe may absorb infrared radiation. The $Fe^{2+}$ ion, when incorporated into a glass or mineral, exhibits an absorption band near 1 $\mu$m,[20] and often a second band near 1.8 $\mu$m.[35] Also, if both $Fe^{2+}$ and $Fe^{3+}$ ions are present and adjacent to one another, the transfer of an electron from $Fe^{2+}$ to $Fe^{3+}$ ("intervalence charge transfer") results in absorption at visible wavelengths.[27]

The characteristic absorption spectra for these two mechanisms may be separated by comparing the measured $k$ values for the mixed oxidation state sample SA10, which shows the effects of both mechanisms, with those of the two fully reduced samples, which show only the direct $Fe^{2+}$ absorption. In Fig. 3, the measured $k$ spectrum for sample SA10 is shown, along with the "residual" spectrum, obtained by subtracting the component attributable to absorption by $Fe^{2+}$. The $Fe^{2+}$ component was determined as the mean value of $k/[Fe^{2+}]$ measured for the two fully reduced samples, multiplied by the $Fe^{2+}$ concentration of slag SA10.

The residual $k$ spectrum consists of an absorption band in the visible, with a tail extending into the infrared, superimposed on a UV absorption edge. The UV absorption edge is due to $Fe^{3+} - O$ charge transfer.[19] The wavelength position of the visible absorption band agrees with the range of wavelengths reported for $Fe^{2+} - Fe^{3+}$ intervalence charge transfer bands in crystalline minerals (0.52–0.77 $\mu$m).[27]

To develop a correlation for $k$, it was assumed that, at infrared wavelengths, $k$ could be written as the sum of two terms describing the infrared tail of the charge transfer band and the absorption due to $Fe^{2+}$, respectively:

$$k(\lambda) = a_1 e^{b/\lambda} + a_2 g(\lambda) \tag{7}$$

The exponent $b$ and the function $g(\lambda)$ are taken to be independent of composition. The function $g(\lambda)$ is taken to be the mean value of $k/[Fe^{2+}]$ for the fully reduced samples. The value of

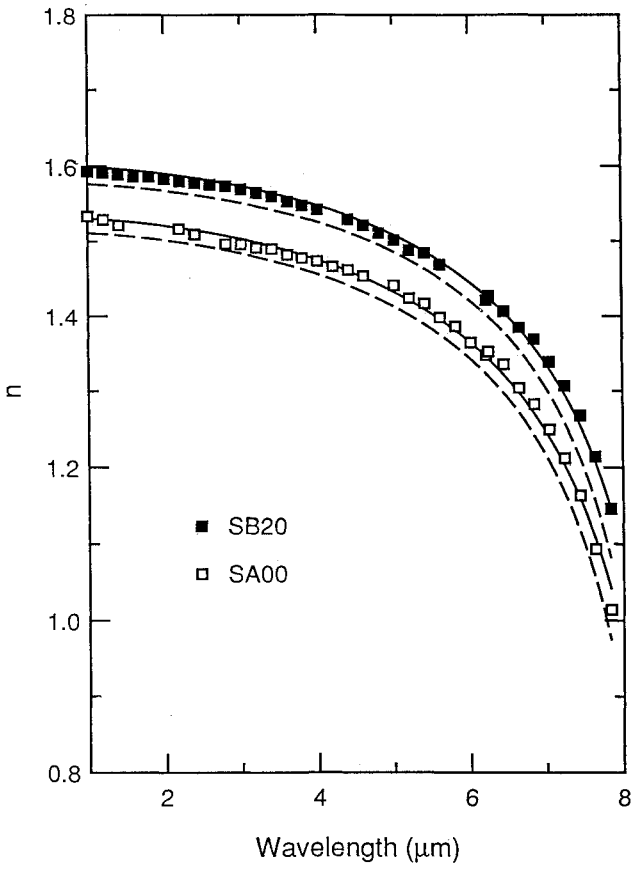


**Fig. 2 Comparison of predicted $n$ with measured values. Dashed curves are computed from Eq. (2) and solid curves from Eq. (5).**

**Table 3 Parameters defining the functions $F_i(\lambda)$ in the mixture rule for $n$ [Eqs. (5) and (6)]**

| Oxide | $a_i$ | $b_i$ | $c_i$ | $d_i$ |
|---|---|---|---|---|
| $SiO_2$ | 0.9389 | 53.00 | 5.001 | 420.0 |
| $Al_2O_3$ | 1.914 | 174.0 | 10.36 | 1634 |
| CaO | 4.250 | 827.7 | 16.63 | 6102 |
| $Fe_2O_3$ | 1.647 | 0.00 | 11.36 | 0.00 |
| $TiO_2$ | 2.720 | 260.0 | 15.80 | 1954 |
| MgO | 1.278 | 136.9 | 7.433 | 1201 |

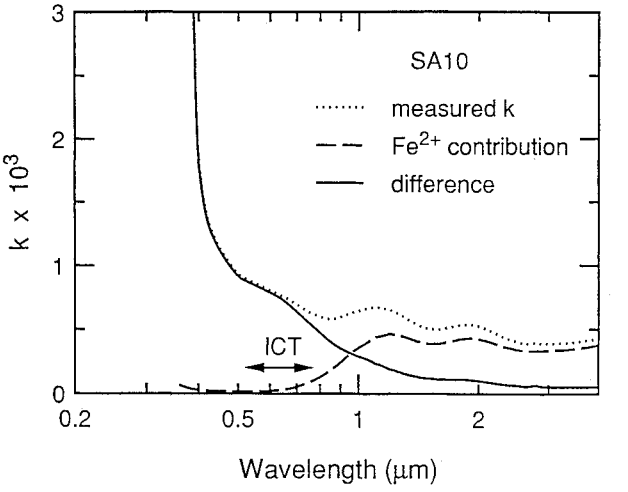


**Fig. 3 Residual $k$ spectrum for sample SA10 obtained by subtracting the $Fe^{2+}$ contribution. The range of $Fe^{2+} - Fe^{3+}$ intervalence charge transfer band positions given by Burns and Vaughan[27] is indicated.**

$b$ was chosen to give the best overall fit to the measured spectra, summed over all samples. The value so determined was $b = 1.75$ μm. The two functions $e^{b/\lambda}$ and $g(\lambda)$ are shown in Fig. 4.

Choosing $a_1$ and $a_2$ for the best fit for each sample, the functional form of Eq. (7) was found to fit the measured data very well, with relative errors usually less than 3%. The set of best-fit values of $a_1$ and $a_2$ determined for each sample were analyzed statistically to determine their correlation with composition. It was found that $a_1$ was strongly correlated with the product $[Fe^{2+}]\,[Fe^{3+}]$, whereas $a_2$ was strongly correlated with $[Fe^{2+}]$, as seen in Fig. 5. Such a composition dependence is not surprising, considering the absorption mechanism to which each coefficient corresponds.

A correlation for $k$ in the wavelength range 0.7–4 μm is obtained by expressing the composition dependence of $a_1$ and $a_2$ by the regression curves shown in Fig. 5 (linear for $a_1$, quadratic for $a_2$). Substituting the regression equations for $a_1$ and $a_2$ into Eq. (7) and recasting the concentrations in terms of the weight percent $Fe_2O_3$ and the ferrous ratio $r$, defined as

$$r = \frac{[Fe^{2+}]}{[Fe^{2+}] + [Fe^{3+}]} \tag{8}$$

yields the expression

$$k(\lambda) = 3.61 \times 10^{-7}\,\rho^2 r(1-r)\,(Fe_2O_3)^2 e^{1.75/\lambda} + \rho r(Fe_2O_3)\,[0.0963 + 0.0011\rho r(Fe_2O_3)]\,g(\lambda) \tag{9}$$

where, as before, $\rho$ is the sample density (g/cm$^3$) and $(Fe_2O_3)$ is the $Fe_2O_3$ weight percent. The error in using Eq. (9) to compute $k$ was found to be usually less than 10%, although the low-Fe samples ($\approx 1\%$ $Fe_2O_3$) showed a greater discrepancy, attributable to some OH absorption seen for these samples, which is not accounted for in Eq. (9). For the samples with more than 1% $Fe_2O_3$, the largest error at any one wavelength in the range 0.7 μm $< \lambda <$ 4.0 μm was 19%, and the largest wavelength-averaged (rms) relative error was 11% (consistent with the scatter seen in Fig. 5). Because the measured values of $k$ ranged over nearly two orders of magnitude, this error is considered acceptable.

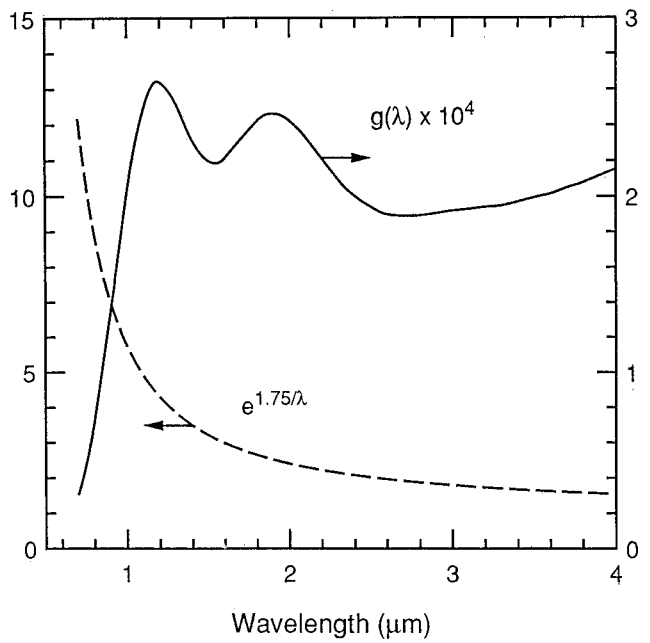


**Fig. 4 The two functions appearing in the correlation for $k$ [Eq. (7)]. The function $e^{1.75/\lambda}$ characterizes the tail of the $Fe^{2+} - Fe^{3+}$ charge transfer band, and the function $g(\lambda)$ characterizes the $Fe^{2+}$ absorption spectrum.**

No effects attributable to Ti could be seen in the $k$ spectra for the four Ti-bearing slags. The correlation equation (9), which neglects $TiO_2$, was found to predict $k$ for the Ti-bearing samples as accurately as for the Ti-free samples. Consequently, it was concluded that the effects of Ti on $k$ may be neglected, at least for $TiO_2$ contents less than $\approx 1\%$.

At wavelengths longer than about 4 μm, all of the slags become strongly absorbing, independent of iron content. The determination of the responsible absorption mechanism in this wavelength region may be made most easily by comparing the measured $k$ values with the known values for the component oxides.

The optical constants for several pure oxides are shown in Fig. 6. The sources for these values are Philipp[36] for fused silica, Toon et al.[11] for $Al_2O_3$, Jacobson and Nixon[31] for CaO, and Bohren and Huffman[13] for MgO. The value of $k$ for fused silica is seen to be much greater than that for the other oxides for wavelengths $\lambda < 10$ μm. In Fig. 7, the $k$ values measured for

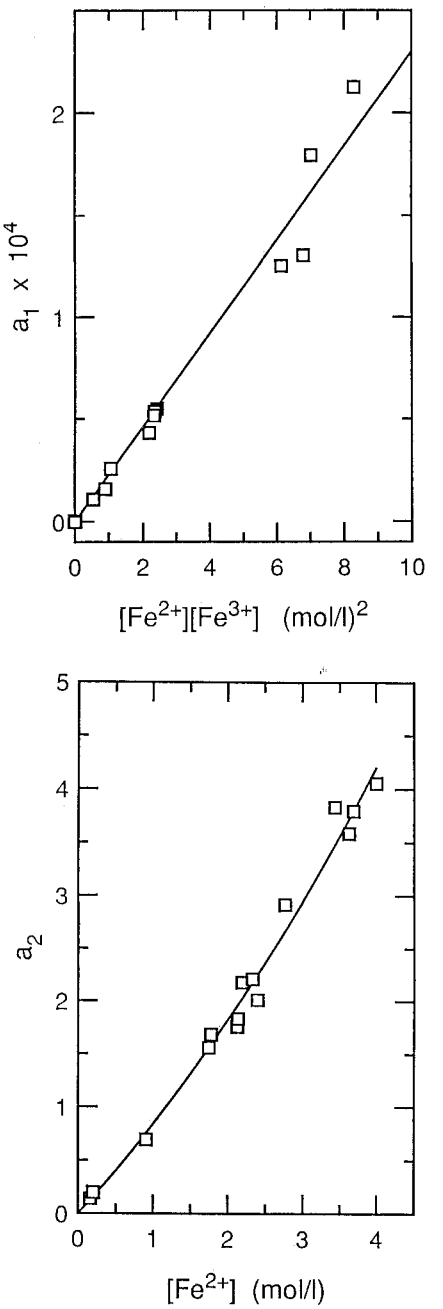


**Fig. 5 Best-fit values of the coefficients $a_1$ and $a_2$ in Eq. (7) vs $[Fe^{2+}]\,[Fe^{3+}]$ and $[Fe^{2+}]$, respectively.**

slag SA00 are compared to the $k$ values for fused silica. The fused silica values scaled by the molar $SiO_2$ content of slag SA00 are also shown. This comparison shows that the absorption in the 4–9-$\mu$m region may be statisfactorily explained as originating from the silica content of the slag. (For slags that contain OH, the OH band near 7 $\mu$m also makes a contribution to $k$ in this wavelength range, as shown in Fig. 1.)

Absorption in this wavelength region (i.e., on the high-frequency side of the highest fundamental vibrational frequency) is due to "multiphonon" absorption, that is, the coupling of two or more vibrational modes to yield combination or overtone bands.[37] Measurements in this spectral region for multicomponent silicate glasses are extremely rare. The present measurements indicate that the processes responsible for absorption are not significantly affected by the presence of the other oxides, except for some degree of smoothing out of the $k$ spectrum. This leads to the conclusion that the value of $k$ in this wavelength range may be estimated by simply scaling the present measured values by the $SiO_2$ content of the slag in question, relative to that of the present work.

At wavelengths beyond 9 $\mu$m, the $k$ values measured for slag SA00 deviate from those for $SiO_2$. The slag remains absorbing at wavelengths near 11 $\mu$m, where the $SiO_2$ absorption has fallen off sharply. At approximately 13 $\mu$m, the slag and fused silica again have similar $k$ values. This behavior is explainable in terms of absorption by $SiO^-$ in the slag, as will be discussed later.

It was found that the optical constants in the 8–13-$\mu$m wavelength range could be reasonably fit by the multiple oscillator model[13]

$$m^2 = n_\infty^2 + \sum_{i=1}^{N} \frac{\omega_{p,j}^2}{\omega_{0,j}^2 - \omega^2 - i\gamma_j\omega} \qquad (10)$$

where $\omega = 1/\lambda$, and the quantities $\omega_{p,j}$, $\omega_{0,j}$, and $\gamma_j$ are the strength, position, and width, respectively, of the $j$th oscillator. Two oscillators were found to be sufficient to describe the 8–12-$\mu$m region, and a third was added to account for the rise in $k$ near 13 $\mu$m. Allowing all parameters (including $n_\infty^2$) to vary for the best fit in the wavelength range 8–13 $\mu$m, the functional form (10) was able to fit the measured optical constants to within about $\pm 0.06$. Typical fits are shown in Fig. 8.

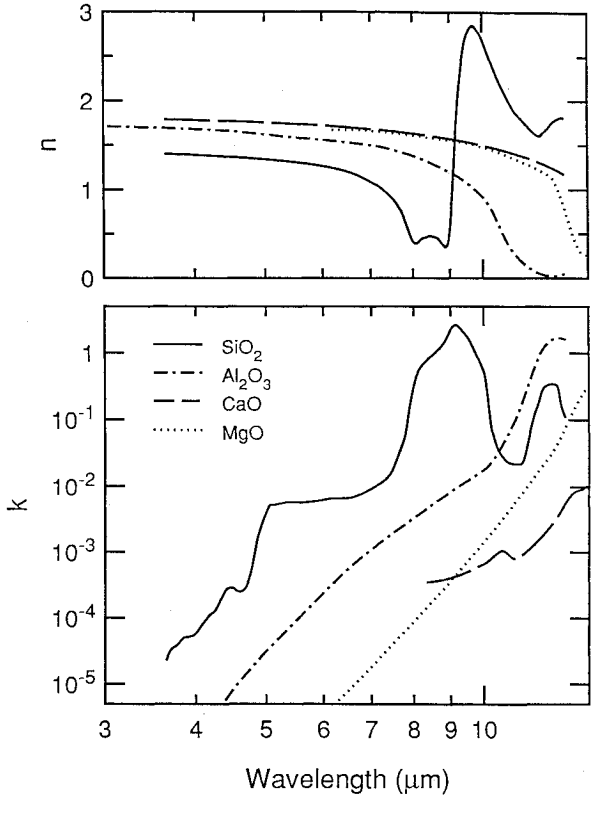


**Fig. 6 Optical constants of $SiO_2$ (fused), $Al_2O_3$, CaO, and MgO.**

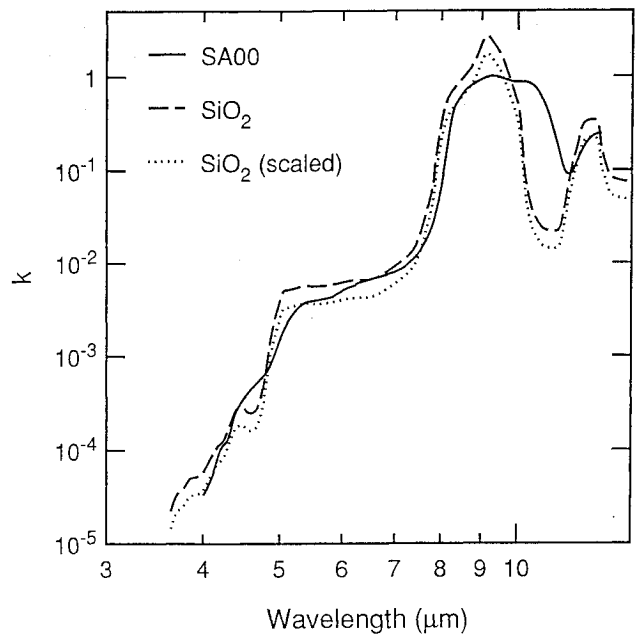


**Fig. 7 Comparison of the $k$ values for slag SA00 with the values for fused silica. The fused silica values scaled by the molar $SiO_2$ content of slag SA00 are also shown.**

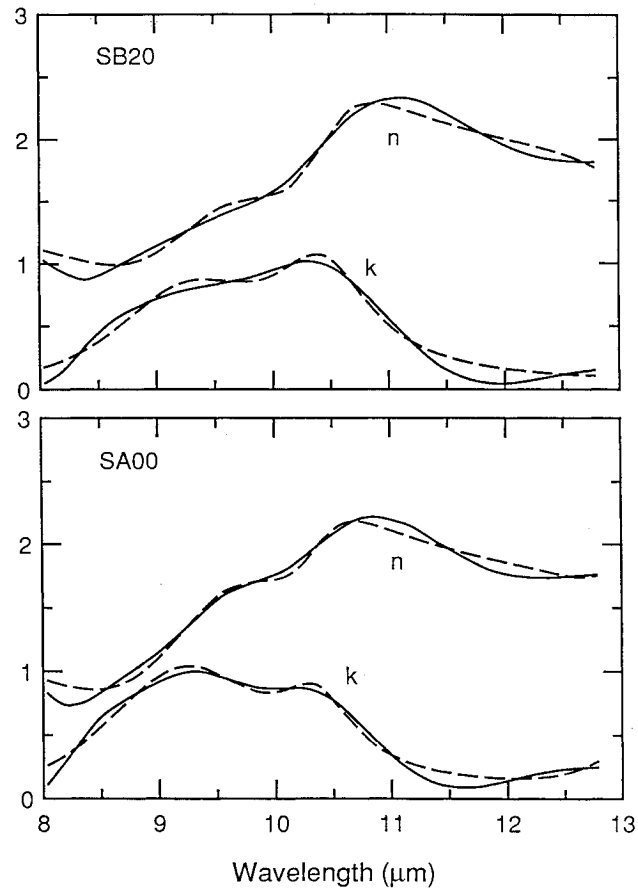


**Fig. 8 Comparison of the three-oscillator fit to the measured optical constants for slags SA00 and SB20. The measured values are shown as the solid curves, and the values computed from Eq. (10) with best-fit parameter values are shown as the dashed curves.**

The peak positions $\omega_{0,j}$ and the widths $\gamma_j$ were found to be nearly the same for each of the slags, with the mean values given in Table 4. The peak positions of the first two oscillators compare favorably with the vibrational frequencies given by Simon[19] for Si-O-Si (bridging oxygen) and Si-O$^-$ (nonbridging oxygen). The frequency range 1065–1100 cm$^{-1}$ is given for the stretching vibration of Si-O-Si, and the range 940–950 cm$^{-1}$ for that of Si-O$^-$, which may be compared with the present values of 1063 cm$^{-1}$ and 956 cm$^{-1}$, respectively. (That these frequencies fall slightly outside the range given by Simon is probably due to the approximate nature of the present fitting procedure.) The mechanism responsible for the feature at 13 $\mu$m is less clear but, for fused silica, the absorption may be due to "ring groups."[19]

The interpretation given here for the responsible absorption mechanisms is strengthened by examining the dependence of the strength $\omega_{p,j}$ on composition. The incorporation of non-network-forming metal anions into the slag (essentially all anions except $Si^{4+}$, $Al^{3+}$, or $P^{5+}$) results in a decrease in the concentration of bridging oxygen, and the formation of nonbridging oxygen. For example, the incorporation of an alkali metal oxide into the slag may be written

$$M_2O + \text{Si-O-Si} \rightarrow 2\ \text{Si-O}^- + 2M^+ \qquad (11)$$

In general, the number $SiO^-$ groups formed is given by charge balance (each $Fe^{2+}$ ion results in two $SiO^-$, as does each $Ca^{2+}$, etc.).

If the interpretation of the absorption peaks as due to Si-O-Si and Si-O$^-$ is correct, the strength of the peak at 1063 cm$^{-1}$ should decrease with increasing non-network-forming oxide content, whereas the strength of the 956 cm$^{-1}$ peak should increase. This effect is shown in Fig. 9, in which the peak strengths for oscillators 1 and 2 (divided by $\omega_0$) are shown vs $Fe_2O_3$ content. (CaO content is approximately constant for these samples.)

The optical constants in the wavelength region 8–13 $\mu$m for the slags of this study may be approximately calculated using Eq. (10) with the average parameter values given in Table 4, along with the average value for $n_\infty^2$ of 2.15 ± 0.08 and the average value for $\omega_{p,3}/\omega_{0,3}$ of 0.053 ± 0.005. The quantities $\omega_{p,1}$ and $\omega_{p,2}$ may be estimated by the straight-line fits in Fig. 9 as

$$\omega_{p,1}/\omega_{0,1} = 0.425 - 0.006(Fe_2O_3) \qquad (12)$$

$$\omega_{p,2}/\omega_{0,2} = 0.175 + 0.0075(Fe_2O_3) \qquad (13)$$

This procedure applies strictly only to slags with the composition studied here. However, it should be possible to include approximately the effects of composition differences using scaling relations (as long as the composition difference is not too extreme). The most significant modification would be to multiply the strengths $\omega_{p,j}$ by the $SiO_2$ concentration of the slag under consideration, relative to the average value for the slags of this study (52%). To use Eqs. (12) and (13) an "effective" $Fe_2O_3$ content may be computed, considering the relative $SiO^-$ concentration compared to that for the slags of this study.

## Summary and Conclusions

The results of an experimental study of the bulk optical constants of coal slags at room temperature have been presented for wavelengths from the visible region to 13 $\mu$m, and the primary physical mechanisms responsible for the optical constants have been discussed.

**Table 4 Average oscillator positions and widths**

| Oscillator | $\bar{\omega}_0$, cm$^{-1}$ | $\bar{\gamma}$, cm$^{-1}$ |
|---|---|---|
| 1 | 1062.8 ± 1.7 | 164.7 ± 3.7 |
| 2 | 955.8 ± 3.1 | 79.1 ± 5.0 |
| 3 | 762.0 ± 5.7 | 27.5 ± 11.0 |

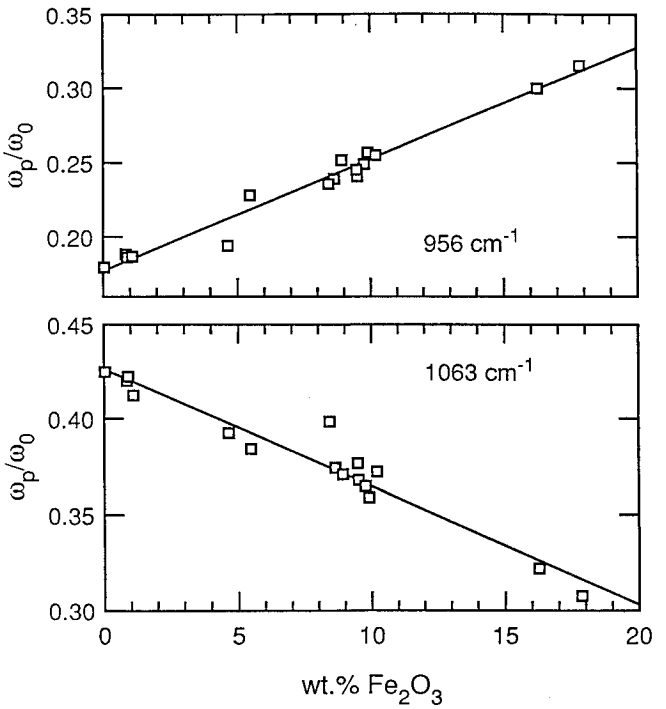


**Fig. 9 Peak strengths for oscillators 1 and 2 (divided by $\omega_0$) vs $Fe_2O_3$ content.**

The imaginary part $k$ of the complex refractive index depends primarily on the iron, silica, and OH content of the slag. Iron is the dominant absorber for $\lambda < 4$ $\mu$m. A correlation was developed for the effects of Fe on $k$ in this wavelength range, accounting for both the dependence on total Fe content and oxidation state. The possible effects of titanium on $k$ were examined and found to be negligible for the range of Ti contents typical for coal slags and ashes. The presence of OH in the slag results in two absorption bands, one near 2.8 $\mu$m and the other near 7 $\mu$m.

The value of $k$ in the longer-wavelength region is found to be determined primarily by the slag silica content. The absorption in the 5–8-$\mu$m region compares well with that of fused silica and appears to be caused primarily by combination and overtone vibrational absorption. In the 8–13-$\mu$m region, the optical constants are determined by the fundamental vibrational resonances of Si-O-Si and Si-O$^-$. A three-oscillator model was found to agree reasonably well with the measured values in this region.

A mixture rule was developed to predict the real part $n$ of the refractive index for the wavelength range 1–8 $\mu$m in terms of the oxide components $SiO_2$, $Al_2O_3$, CaO, MgO, $TiO_2$, and $Fe_2O_3$. At longer wavelengths, $n$ may be computed along with $k$ from the three-oscillator model.

The data presented here should allow inclusion of more realistic optical constants for fly ash into computational models of radiative heat transfer in coal combustion systems. In particular, these data make possible consideration of the strong wavelength dependence of the optical constants and allow consideration of the effects of ash composition on heat transfer. The results of our measurements of the temperature dependence of the $k$ will be presented shortly, as will our theoretical investigations of the implications of these results for heat transfer. A complete summary of this work, including tabulated optical constants, is available in the thesis by Goodwin.[22]

## Acknowledgments

This work was supported by the National Science Founation under Grant MEA-82-12075. We would like to thank Professor Sidney Self for many helpful discussions regarding this work and Mr. Jon Ebert, who assisted in acquiring some of the data.

## References


[1]Wall, T. F., Lowe, A., Wibberly, L. J., and Stewart, I., "Mineral Matter in Coal and the Thermal Performance of Large Boilers," *Progress in Energy and Combustion Science,* Vol. 5, 1979, pp. 1-29.

[2]Sarofim, A. F., "Flame Emissivities: Alternative Fuels," *Progress in Astronautics and Aeronautics: Combustion and Chemical Kinetics,* Vol. 62, edited by C. T. Bowman and J. Birkeland, AIAA, New York, 1978.

[3]Viskanta, R. and Kim, D. M., "Heat Transfer through Irradiated, Semi-Transparent Layers at High Temperature," *Journal of Heat Transfer,* Vol. 102, 1980, pp. 182-184.

[4]Willis, C., "The Complex Refractive Index of Particles in a Flame," *Journal of Physics D: Applied Physics,* Vol. 3, 1970, pp. 1944-1956.

[5]Volz, F. E., "Infrared Optical Constants of Ammonium Sulfate, Sahara Dust, Volcanic Pumice, and Flyash," *Applied Optics,* Vol. 12, 1973, pp. 564-568.

[6]Lowe, A., Stewart, I. M., and Wall, T. F., "The Measurement and Interpretation of Radiation from Fly Ash Particles in Large Pulverized Coal Flames," *Proceedings of the Seventeenth Symposium (International) on Combustion,"* The Combustion Institute, Pittsburgh, PA, 1979, pp. 105-112.

[7]Cowen, S. J., Ensor, D. S., and Sparks, L. S., "The Relationship of Fly Ash Light Absorption to Smoke Plume Opacity," *Atmospheric Environment,* Vol. 15, 1981, pp. 2091-2096.

[8]Gupta, R. P. and Wall, T. F., "The Optical Properties of Fly Ash in Coal Fired Furnaces," *Combustion and Flame,* Vol. 61, 1985, pp. 145-151.

[9]Wyatt, P. J., "Some Chemical, Physical, and Optical Properties of Fly Ash Particles," *Applied Optics,* Vol. 19, 1980, pp. 975-983.

[10]Gupta, R. P. and Wall, T. F., "The Complex Refractive Index of Particles," *Journal of Physics D: Applied Physics,* Vol. 14, 1981, pp. L95-98.

[11]Toon, O. B., Pollack, J. B., and Khare, B. N., "The Optical Constants of Several Atmospheric Aerosol Species: Ammonium Sulfate, Aluminum Oxide, and Sodium Chloride," *Journal of Geophysical Research,* Vol. 81, 1976, pp. 5733-5748.

[12]Marx, E., "Data Analysis for Size and Refractive Index Determination from Light Scattering by Single Spheres," *Aerosol Science and Technology,* Vol. 2, 1983, p. 190.

[13]Bohren, C. T. and Huffman, D. R., *Absorption and Scattering of Light by Small Particles,* Wiley, New York, 1983.

[14]Gerber, H. E. and Hindman, E. E., "Light Absorption by Aerosol Particles: First International Workshop," *Applied Optics,* Vol. 21, 1982, p. 370.

[15]Steyer, T. R., Day, K. L., and Huffman, D. R., "Infrared Absorption by Small Amorphous Quartz Spheres," *Applied Optics,* Vol. 13, 1974, pp. 1586-1590.

[16]Bergstrom, R. W., "Extinction and Absorption Coefficients of the Atmospheric Aerosol as a Function of Particle Size," *Beiträge zur Physik der Atmosphäre,* Vol. 46, 1973, pp. 223-234.

[17]Wall, T. F., Lowe, A., Wibberly, L. J., Mai-Viet, T., and Gupta, R. P., "Fly Ash Characteristics and Radiative Heat Transfer in Pulverized-Coal-Fired Furnaces," *Combustion Science and Technology,* Vol. 26, 1981, pp. 107-121.

[18]Prentice, B. A., Fisher, G. L., Lai, C. E., and Hayes, T. L., "Correlation of Light Microscopic Morphologic Analysis with SEM X-Ray Analysis of Individual Coal Fly Ash Particles," *Aerosol Science and Technology,* Vol. 2, 1983, p. 252.

[19]Simon, I., "Infrared Studies of Glasses," *Modern Aspects of the Vitreous State,* Vol. 1, edited by J. D. MacKenzie, Butterworths, Washington, 1960.

[20]Bates, T., "Ligand Field Theory and Absorption Spectra of Transition-Metal Ions in Glasses," *Modern Aspects of the Vitreous State,* Vol. 2, edited by J. D. MacKenzie, Butterworths, London, 1962.

[21]Pollack, J. B., Toon, O. B., and Khare, B. N., "Optical Properties of Some Terrestrial Rocks and Glasses," *Icarus,* Vol. 19, 1973, pp. 372-389.

[22]Goodwin, D. G., Ph.D. Thesis, Stanford Univ., Stanford, CA, HTGL Rept. T-255, 1986 (unpublished).

[23]Plante, E. R. and Cook, L. P., "Compositional Modeling of MHD Channel Slag, with Preliminary Vapor Pressure Data," *Proceedings of the 17th Symposium on the Engineering Aspects of Magnetohydrodynamics,* 1978, pp. C.1.1-C.1.6.

[24]Goodwin, D. G. and Mitchner, M., "Measurements of the Near Infrared Optical Properties of Coal Slags," *Chemical Engineering Communications,* Vol. 44, 1986, pp. 241-255.

[25]Marfunin, A. S., *Spectroscopy, Luminescence and Radiation Centers in Minerals,* Springer-Verlag, Berlin, 1979.

[26]Malitson, I. H., "Refraction and Disperson of Synthetic Sapphire," *Journal of the Optical Society of America,* Vol. 52, 1962, pp. 1377-1379.

[27]Burns, R. G. and Vaughan, D. J., "Polarized Electronic Spectra," *Infrared and Raman Spectroscopy of Lunar and Terrestrial Minerals,* edited by C. Karr Jr., Academic Press, New York, 1975.

[28]Robinson, J. W. (Ed.), *CRC Handbook of Spectroscopy,* Vol. 2, CRC Press, Cleveland, OH, 1974, p. 71.

[29]Born, M. and Wolf, E., *Principles of Optics,* 6th ed., Pergamon Press, Oxford, 1980.

[30]Malitson, I. H., "Interspecimen Comparison of the Refractive Index of Fused Silica," *Journal of the Optical Society of America,* Vol. 55, 1965, pp. 1205-1209.

[31]Jacobson, J. L. and Nixon, E. R., "Infrared Dielectric Response and Lattice Vibrations of Calcium and Strontium Oxides," *Journal of the Chemistry and Physics of Solids,* Vol. 29, 1968, pp. 967-976.

[32]Bailey, P. C., "Absorption and Reflectivity Measurements on Some Rare Earth Iron Garnets and $\alpha - Fe_2O_3$," *Journal of Applied Physics,* Vol. 31, 1960, pp. 395-405.

[33]DeVore, J. R., "Refractive Indices of Rutile and Sphalerite," *Journal of the Optical Society of America,* Vol. 41, 1951, pp. 417-419.

[34]Wolf, W. L., "Properties of Optical Materials," *Handbook of Optics,* edited by W. G. Driscoll, McGraw-Hill, New York, 1978.

[35]Goldman, D. S. and Berg, J. I., "Spectral Study of Ferrous Iron in Ca-Al-borosilicate Glass at Room and Melt Temperatures," *Journal of Non-Crystalline Solids,* Vol. 38, 1980, pp. 183-188.

[36]Philipp, H. R., "Silicon Dioxide ($SiO_2$) (glass)," *Handbook of Optical Constants of Solids,* edited by E. D. Palik, Academic Press, New York, 1985.

[37]Bendow, B., "Multiphonon Infrared Absorption in the Highly-Transparent Frequency Regime of Solids," *Solid State Physics,* Vol. 33, Academic Press, New York, 1978.